OPEN

LFZ-4-46, a tetrahydroisoquinoline derivative, induces apoptosis and cell cycle arrest via induction of DNA damage and activation of MAPKs pathway in cancer cells

Lili Xu[a,*],Guozheng Huang[b,c,*], Zhihui Zhu[a], Shasha Tian[a], Yingying Wei[a], Huanwu Hong[a], Xiaowei Lu[a], Ying Li[b], Feize Liu[b] and Huajun Zhao[a]

LFZ-4-46, that is [2-hydroxy-1-phenyl-1,5,6,10b-tetrahydropyrazolo(5,1-a) isoquinolin-3(2*H*)-yl](phenyl) methanone, a tetrahydroisoquinoline derivative with a pyrazolidine moiety, was synthetically prepared. The anti-cancer mechanism of the compound has not been clarified yet. In this study, the anticancer effects and potential mechanisms of LFZ-4-46 on human breast and prostate cancer cells were explored. (a) 3-(4,5-Dimethyl-2-thiazolyl)-2,5-diphenyl-2H-tetrazoliumbromide assay was first performed to detect the effects of LFZ-4-46 on the viability of human cancer cells. (b) Comet assay was utilized to evaluate DNA damage. (c) Cell cycle, apoptosis and mitochondrial membrane potential were detected by flow cytometry. (d) The expression of relative proteins was detected by western blotting assay. LFZ-4-46 significantly inhibited the viability of cancer cells in a time- and dose-dependent manner and had no obviously inhibitory effect on the viability of mammary epithelial MCF-10A cells. Mechanistic studies demonstrated that LFZ-4-46-induced cell apoptosis and cycle arrest were mediated by DNA damage. It caused DNA damage through activating γ-H2AX and breaking DNA strands. Further studies showed that mitogen-activated protein kinasess pathway was involved in these activated several key molecular events. Finally, LFZ-4-46 showed a potent antitumor effect *in vivo*. These results suggest that LFZ-4-46 may be a potential lead compound for the treatment of breast and prostate cancer. *Anti-Cancer Drugs* 32: 842–854 Copyright © 2021 The Author(s). Published by Wolters Kluwer Health, Inc.

Anti-Cancer Drugs 2021, **32**:842–854

Keywords: apoptosis, cell cycle, DNA damage, LFZ-4-46, mitogen-activated protein kinases pathway

[a]Department of Pharmacy, College of Pharmaceutical Sciences, Zhejiang Chinese Medical University, Hangzhou, [b]Xinjiang Technical Institute of Physics and Chemistry, Chinese Academy of Sciences, Xinjiang and [c]Department of Chemical Engineering, College of Chemistry and Chemical Engineering, Anhui University of Technology, Ma'anshan, China

Correspondence to Huajun Zhao, PhD, Zhejiang Chinese Medical University,Hangzhou 310053, China
Tel: +86 571 61768141; e-mail: zhj@zcmu.edu.cn

*These authors contributed equally to this article.

Received 21 December 2020 **Revised form accepted** 19 March 2021

Introduction

Cancer has an impact on health-related quality of human life. Human health is threatened by some common cancer, such as breast cancer and prostate cancer. Breast cancer is one of the most common malignant tumors and vital causes of death in women [1]. The incidence of breast cancer worldwide has increased by an average of 3% a year over the past decade [2]. Also, the incidence rate of prostate cancer is the highest in men in developed countries and the eighth leading cause of cancer death globally [3]. Therefore, it is urgent to find a new agent that can effectively treat breast and prostate cancer.

LFZ-4-46 (Fig. 1a), that is [2-hydroxy-1-phenyl-1,5,6,10b-tetrahydropyrazolo(5,1-a)isoquinolin-3(2*H*)-yl](phenyl) methanone, a tetrahydroisoquinoline derivative with a pyrazolidine moiety, was synthetically prepared. Nitrogen-containing heterocyclic molecules are one of the largest components of chemical entities [4–6]. Tetrahydroisoquinoline and its derivatives are an extremely privileged heterocyclic class, which have antitumor, antibacterial and other biological properties [7–10]. It became a common synthetic target in organic synthesis. Also, the substitution of the C1 position in the tetrahydroisoquinoline nucleus can bring useful derivatives [11–14]. Then, pyrazolidines are *N*-heterocyclic compounds with an N–N single bond. The research on the cytotoxic activity of pyrazolidine has become a hot topic [15–17]. Interestingly, two important scaffold combination may show good biological activity. As far as we know, the activity of this compound containing the two important scaffolds has so far not been intensively investigated. On this basis, we suppose that LFZ-4-46, a tetrahydroisoquinoline derivative with a pyrazolidine moiety, has good anticancer activity.

In this study, we found that LFZ-4-46 could effectively inhibit the viability of different human cancer cells and had the strongest inhibitory effect on the growth of breast

0959-4973 Copyright © 2021 The Author(s). Published by Wolters Kluwer Health, Inc. DOI: 10.1097/CAD.0000000000001077

Fig. 1

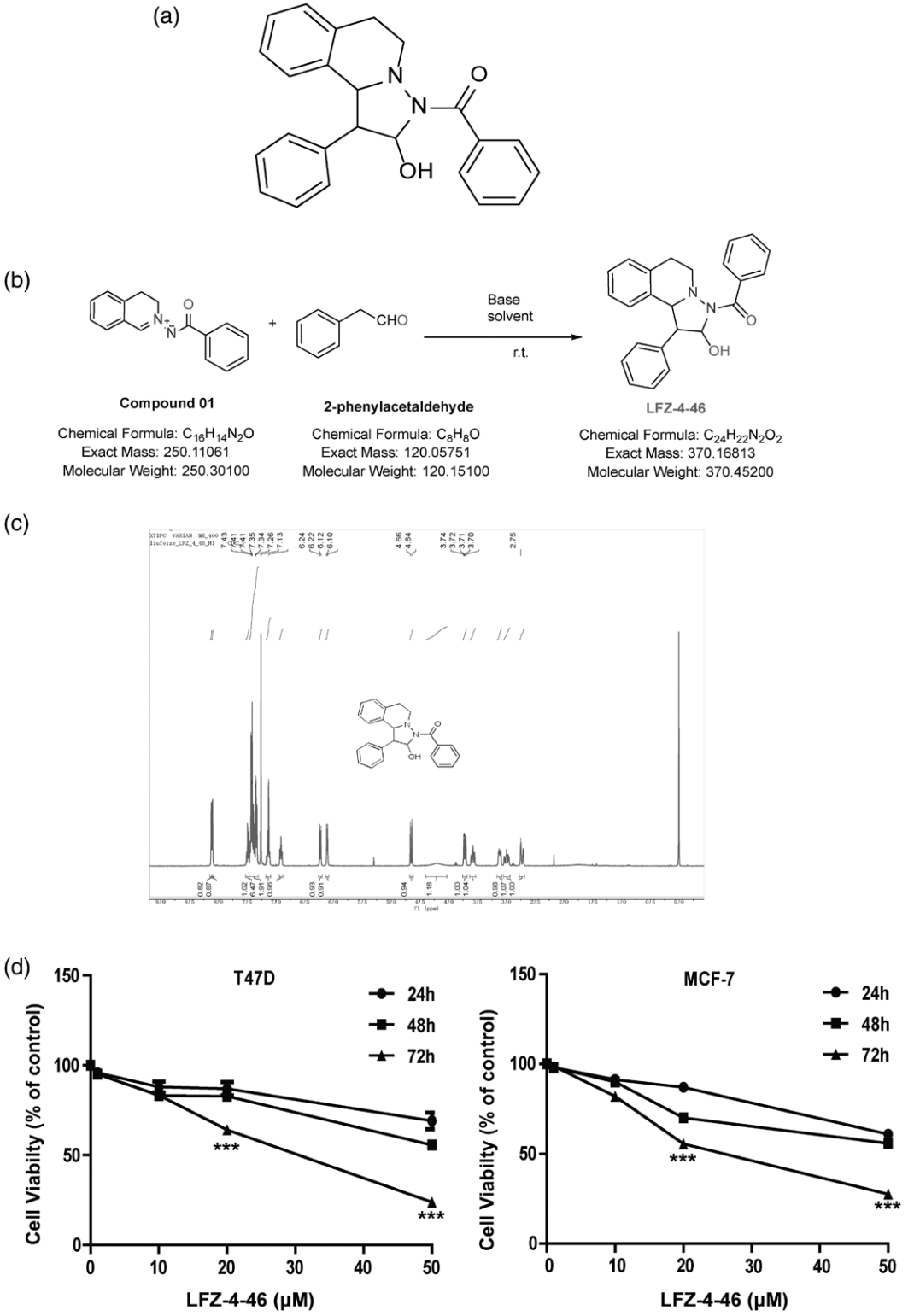

The inhibitory effect of [2-hydroxy-1-phenyl-1,5,6,10b-tetrahydropyrazolo(5,1-a)isoquinolin-3(2*H*)-yl](phenyl) (LFZ-4-46) on the viability of human cancer cells. (a) Chemical structure of LFZ-4-46. (b) The synthesis method of LFZ-4-46. (c) The NMR data of LFZ-4-46. (d) Breast cancer T47D cells and prostate cancer PC3 cells were treated with indicated concentrations of LFZ-4-46 for 24, 48 and 72 h. Cell viability was detected by 3-(4,5-Dimethyl-2-thiazolyl)-2,5-diphenyl-2H-tetrazoliumbromide (MTT) assay. Data are presented as the mean ± SD of at least three independent experiments. *** $P<0.001$. NMR, nuclear magnetic resonance

and prostate cancer cells. Related mechanistic studies have found that LFZ-4-46 activated the caspase-dependent apoptosis pathway, leading to cell cycle arrest at the G2/M phase through induction of DNA damage and activation of mitogen-activated protein kinases (MAPKs) pathway. Our data suggest that LFZ-4-46 may be a novel lead compound to provide guidance for the next formation of the same type of compounds.

Materials and methods

Chemicals

LFZ-4-46 was first appeared in the article by Studer *et al.* (*Chem. Sci.*, 2015, 6, 1252–1257). They treated the benzoyl(3,4-dihydroisoquinolin-2-ium-2-yl)amide (compound 01) and phenylacetaldehyde in the presence of 1,4-dimethyl-1*H*-1,2,4-triazol-4-ium iodide and 1,8-Diazabicyclo[5.4.0] undec-7-ene, with 3,3′,5,5′-tetra-*tert*-butyldiphenoquinon as the oxidant to yield LFZ-4-46. We recently found that only with a base, the reaction will work smoothly to afford the target compound. ^{1}H nuclear magnetic resonance (NMR) (400 MHz, $CDCl_3$) δ 8.11 (d, *J* = 7.5 Hz, 2H), 7.51–7.32 (m, 7H), 7.17–7.07 (m, 2H), 6.91 (dd, *J* = 11.1, 5.0 Hz, 1H), 6.23 (d, *J* = 7.7 Hz, 1H), 6.11 (d, *J* = 3.5 Hz, 1H), 4.65 (d, *J* = 11.0 Hz, 1H), 4.26 (s, 1H), 3.72 (dd, *J* = 11.0, 5.7 Hz, 1H), 3.62–3.54 (m, 1H), 3.11 (m, 1H), 3.04–2.94 (m, 1H), 2.72 (d, *J* = 16.0 Hz, 1H). The NMR data can be seen in Fig. 1b–c. LFZ-4-46 was maintained at –80 °C in the dark or dissolved by dimethyl sulfoxide (DMSO) and stored at –20 °C (used *in vitro*) as stock solutions. The stock solutions were diluted to the desired concentrations in a complete medium immediately prior to each experiment. The final concentration of DMSO did not exceed 0.1%. For in-vivo studies, LFZ-4-46 was dissolved in PBS/Cremophor EL/ethanol (90: 5: 5; Cremophor EL from Sigma-Aldrich, St Louis, Missouri, USA).

Cell culture and reagents

The T47D, PC3, DU-145, SGC-7901 and MCF-10A cell lines were purchased from the Cell Bank of the Institute of Biochemistry and Cell Biology, Chinese Academy of Sciences (Shanghai, China) and stored in liquid nitrogen. Cells were cultured in Dulbecco's modified Eagle's medium (DMEM) culture medium containing 10% fetal bovine serum (FBS; both from Gibco, USA), 100 U/ml penicillin G, 2.5 μg/ml amphotericin B and 100 μg/ml streptomycin (complete medium) at 37°C with 5% CO_2 in a humidified atmosphere.

3-(4,5-Dimethyl-2-thiazolyl)-2,5-diphenyl-2H-tetrazo- liumbromide (MTT) and DMSO were purchased from Sigma-Aldrich. Propidium iodide/RNase staining kit and Annexin V-fluorescein isothiocyanate (FITC)/7AAD kit were purchased from BD Pharmingen (SanDiego, California, USA). Inhibitors Z-VAD-FMK (#60332), SB203580 (#5633), SP600125 (#8177) and PD98059 (#9900) were purchased from cell signaling technology (Boston, USA). Antibodies against poly ADP-ribose polymerase (PARP) (#9532), caspase-8 (#4790), cleaved caspase-9 (Asp330, #9501), cleaved caspase-3 (Asp175, #9664), cleaved caspase-7 (#9491), cdc2 (#9116), Cyclin B1 (#12231), p-JNK (#4668), JNK1 (#3708), JNK2 (#4672), p-p38 (#9212), p-ERK (#9101), ERK (#9102), β-tubulin (#2128) and horseradish peroxidase-conjugated secondary antibodies were purchased from Cell Signaling Technologies (Beverly, Massachusetts, USA). γ-H2AX was purchased from Abcam (Cambridge, UK).

Cell viability assay

The effect of LFZ-4-46 on the viability of cells was determined by using the MTT assay. T47D, PC3, DU145, SGC-7901 and MCF-10A cells were placed into 96-well cell culture plates at a final concentration of 5×10^3 cells/well in medium, allowing these cells to attach for 24 h. After treatment with a range of concentration of LFZ-4-46 for 24, 48 or 72 h, 20 μl MTT solution (5 mg/ml) was added for 4 h at 37 °C in the dark and dissolved in 150 μl DMSO. The relative viability of cell was detected by scanning with a cell Imaging Multi-mode Reader (BioTekCA, USA) using a 570 nm filter. The value of IC_{50} was calculated by GraphPad Prism 5.0 software (Graph Pad Software, California, USA).

Apoptosis assay with annexin V-fluorescein isothiocyanate/7-AAD staining

Quantification of apoptotic cells was performed using an Annexin V-FITC Apoptosis Detection Kit (BD Pharmingen, USA). Cells were placed into 6-well plates and treated with LFZ-4-46 for 24 h. Then, cells were collected and resuspended in 500 μl of binding buffer, 5 μl of Annexin V-FITC and 5 μl of propidium iodide staining d for 15 min. Apoptosis results were analyzed by the Guava Easy Cytometer (Guava Technologies, Merck Drugs & Biotechnology, Darmstadt, Germany).

Evaluation of mitochondrial membrane potential (Δψm)

Cells (2×10^5 cells/well) were seeded into 6-well plates and treated with LFZ-4-46 for 24 h before the experiment. After treatment with 10, 20 and 30 μM LFZ-4-46, cells were harvested, washed twice with ice-cold PBS and incubated with JC-1 (10 μg/ml) and then analyzed by flow cytometry.

DAPI staining for cell nuclei

Cells (1×10^5 cells/well) were placed into 6-well plates and with the treatment with LFZ-4-46 for 24 h. The cells were washed with PBS, fixed with 4% paraformaldehyde for 1 h at room temperature, and incubated with 2-(4-Amidinophenyl)-6-indolecarbamidine dihydrochloride (DAPI) (1 μg/ml) for analysis cell apoptosis. Cells with condensed and fragmented DNA (apoptotic cells) were evaluated under a fluorescence microscope (Nikon, Tokyo, Japan).

Comet assay

Cells (1×10^5 cells/well) were placed into 6-well plates. With the treatment of LFZ-4-46 for 24 h, cells were harvested in ice-cold PBS. In combination with low-melting agarose (0.8% w/v, A9414, Sigma-Aldrich, 37 °C 1 g in 100 mL dH_2O), the cells were spread on the comet slide at a ratio of 1:10 (v/v). The slides were solidified in dark at 4 °C for 30 min, immersed in a neutral electrolytic buffer at 4 °C overnight and then electrophoresed at 1.0 V/cm for 30 min after lysis. The lysed sections were placed in 70% ethanol, dried at 37 °C for 15 min, dark stained with ethidium bromide for 20 min and then observed under a fluorescence microscope (Nikon, Tokyo, Japan).

Cell cycle analysis

Cells (3×10^5 cells/well) were plated in 6-well plates and treated with the indicated concentrations of LFZ-4-46 for 24 h. Cells were harvested, washed twice with ice-cold PBS, and fixed in 70% ethanol at 4 °C overnight. Then they were stained with propidium iodide/RNase (0.5 ml/test, 1×10^6 cells) and analyzed after 15 min at room temperature. The samples were analyzed by a flow cytometer (Guava Technologies, Merck Drugs & Biotechnology, Germany), and the DNA content was quantified using modfit software.

Western blotting analysis

The cells treated with LFZ-4-46 were incubated and lysed in radio immunoprecipitation assay buffer containing protease inhibitors (1 mM benzyl alcohol sulfonyl fluoride and 1 μg/ml albumin peptone) and phosphatase inhibitors (1 mM sodium fluoride and 1 mM sodium orthovanadate). Then, the same amount of denatured protein was separated by SDS-PAGE and transferred to the poly (1,1-difluoroethylene) membrane (Millipore, Massachusetts, USA). Then, the membrane with 5% skimmed milk was sealed and incubated with the corresponding primary antibody overnight at 4 °C. The membranes were washed three times with Tris-buffered saline-5% Tween 20 solution, incubated with a horseradish peroxidase-conjugated secondary antibody at room temperature for 2 h, and performed chemiluminescence detection with ECL (Bio-Rad, USA).

Xenograft mouse model

A mouse xenograft model was established to confirm the antitumor effect of LFZ-4-46 *in vivo*. PC3 cells (5×10^6 cells, 0.1 ml DMEM/F12 medium) were injected subcutaneously into 4-week-old BALB/c male nude mice (Shanghai Experimental Animal Center, Shanghai, China). When the tumor volume reached 50 mm^3, the mice were randomly divided into three groups (CremophorEL: Ethanol: Saline = 5:5:90). LFZ-4-46 15 or 30 mg/kg were administered by i.p. injection three times a week for 16 days. The tumor growth was measured every other day, the tumor size was calculated as follows: volume = (width^2 × length)/2. After 16 days, the mice were sacrificed and the xenografts were removed for immunohistochemical analysis. This study was approved by the Institutional Animal Care and Use Committee of Zhejiang Chinese Medical University and was conducted in accordance with the guidelines proposed by the Laboratory Animal Research Center of Zhejiang Chinese Medical University.

Immunohistochemical assay

Immunohistochemistry was performed to detect the expression of γ-H2AX, ERK1/2, p-ERK1/2, JNK1/2, p-JNK1/2 and p-p38. The tissue was fixed with 10% formalin and embedded in paraffin. Sections were dewaxed and rehydrated, and then endogenous peroxidase was blocked with the hydrogen peroxide. Antigen retrieval was performed by exposing the slides in citrate buffer. Afterward, nonspecific immunoglobulin binding was blocked by incubating with 5% albumin cattle (AMRESCO, USA). The primary antibody was incubated overnight at 4 °C, and the slides were incubated in HRP-labeled polymer, stained with Novolink TM Polymer Detection System (ZSGB-BIO, China), and stained with hematoxylin. The image was taken with an Olympus microscope.

Statistical analysis

Data were given as mean ± SD. Statistical significance was analyzed using Student's *t*-test. The criterion of statistical significance was * $P<0.05$, ** $P<0.01$, *** $P<0.001$

Results

LFZ-4-46 inhibited the viability of cancer cells

To investigate the effect of LFZ-4-46 on cell viability, several human cancer cell lines were detected, including T47D (breast cancer), PC3 and DU145 (prostate cancer), SGC-7901 (gastric cancer) and human mammary epithelial cell line MCF-10A. Cell viability was assessed by MTT assay. Our results showed that LFZ-4-46 significantly inhibited the viability of cancer cell lines (IC_{50} were shown in Table 1), especially on cancer cell lines T47D (IC_{50} 26.73 μM) and PC3 (IC_{50} 23.81 μM). These

Table 1 Effects of LFZ-4-46 on the viability of human cancer cells and IC50 values for 72 h were shown in.

Cell lines	IC_{50} (μM, 72 h)
T47D	26.73 ± 1.77
SGC-7901	94.25 ± 1.9
PC3	23.8 ± 1.46
DU145	36.44 ± 4.69
MCF-10A	>50

Table 2 T47D and PC3 cells were treated with indicated concentrations of LFZ-4-46 for 24, 48 and 72 h.

	IC_{50} (μM)	
Times (h)	T47D	PC3
24	90.00 ± 3.96	69.05 ± 4.92
48	73.67 ± 1.17	45.6 ± 0.04
72	26.73 ± 1.77	23.8 ± 1.46

Fig. 2

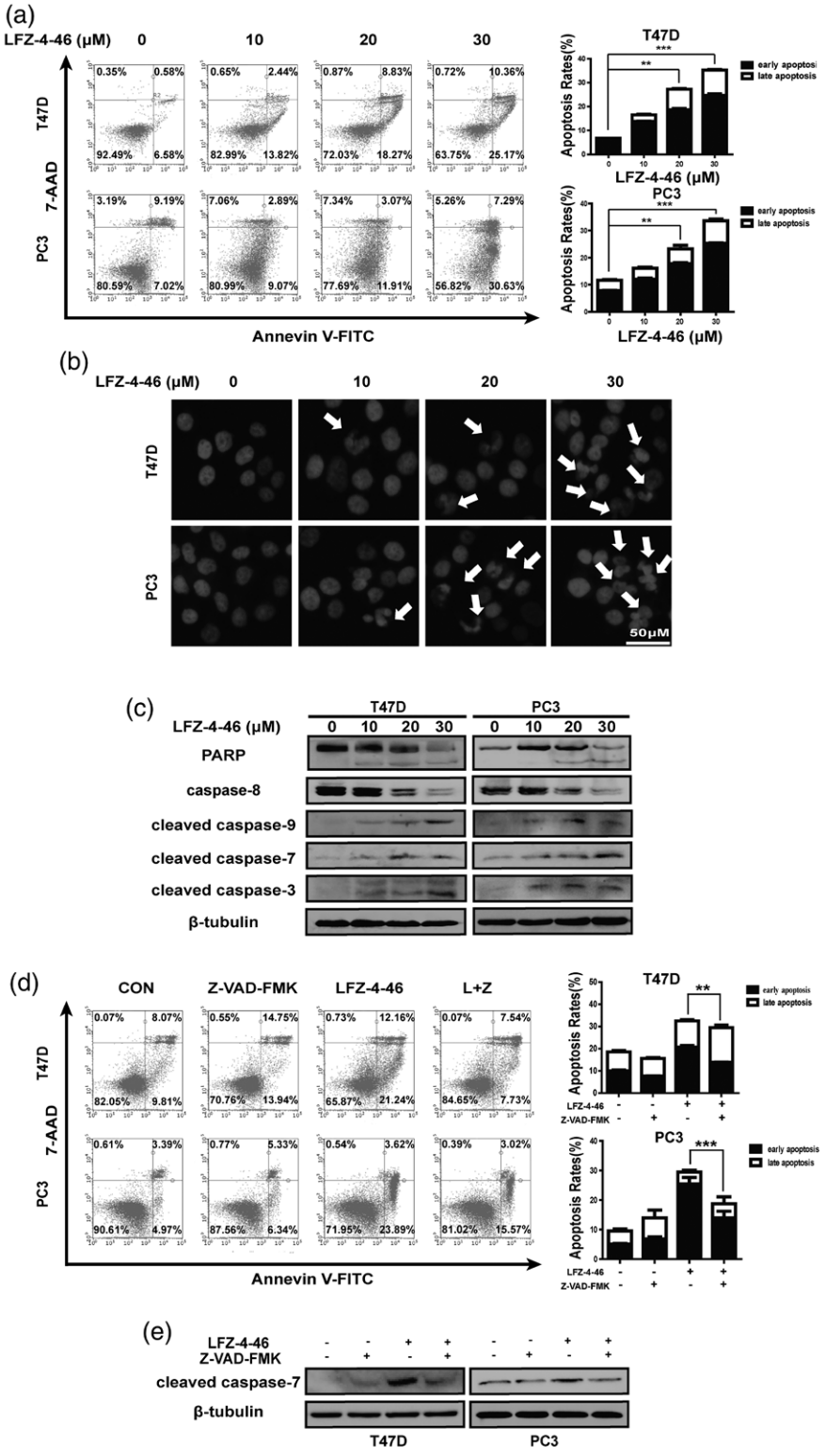

[2-hydroxy-1-phenyl-1,5,6,10b-tetrahydropyrazolo(5,1-a)isoquinolin-3(2*H*)-yl](phenyl) (LFZ-4-46) induced apoptosis in T47D and PC3 cells by activating the caspase pathway. (a) After Annexin V-fluorescein isothiocyanate (FITC)/7AAD staining, the index of apoptotic cells was analyzed by flow cytometry. (b) DAPI staining was used to stain the nucleus after LFZ-4-46 treatment. (c) Western blotting analysis of caspase-related proteins in T47D and PC3 cells. T47D and PC3 cells were treated with LFZ-4-46 (30 μM) for 24 h after pretreatment with caspase inhibitor Z-VAD-FMK (10 μM) for 2 h. After Annexin V-FITC/7AAD staining, the index of apoptotic cells was analyzed by flow cytometry (d). Western blotting analyzed the expression levels of cleaved caspase-7 (e). Data are presented as the mean ± SD of at least three independent experiments. ** $P<0.01$, *** $P<0.001$. DAPI, 2-(4-Amidinophenyl)-6-indolecarbamidine dihydrochloride.

Fig. 3

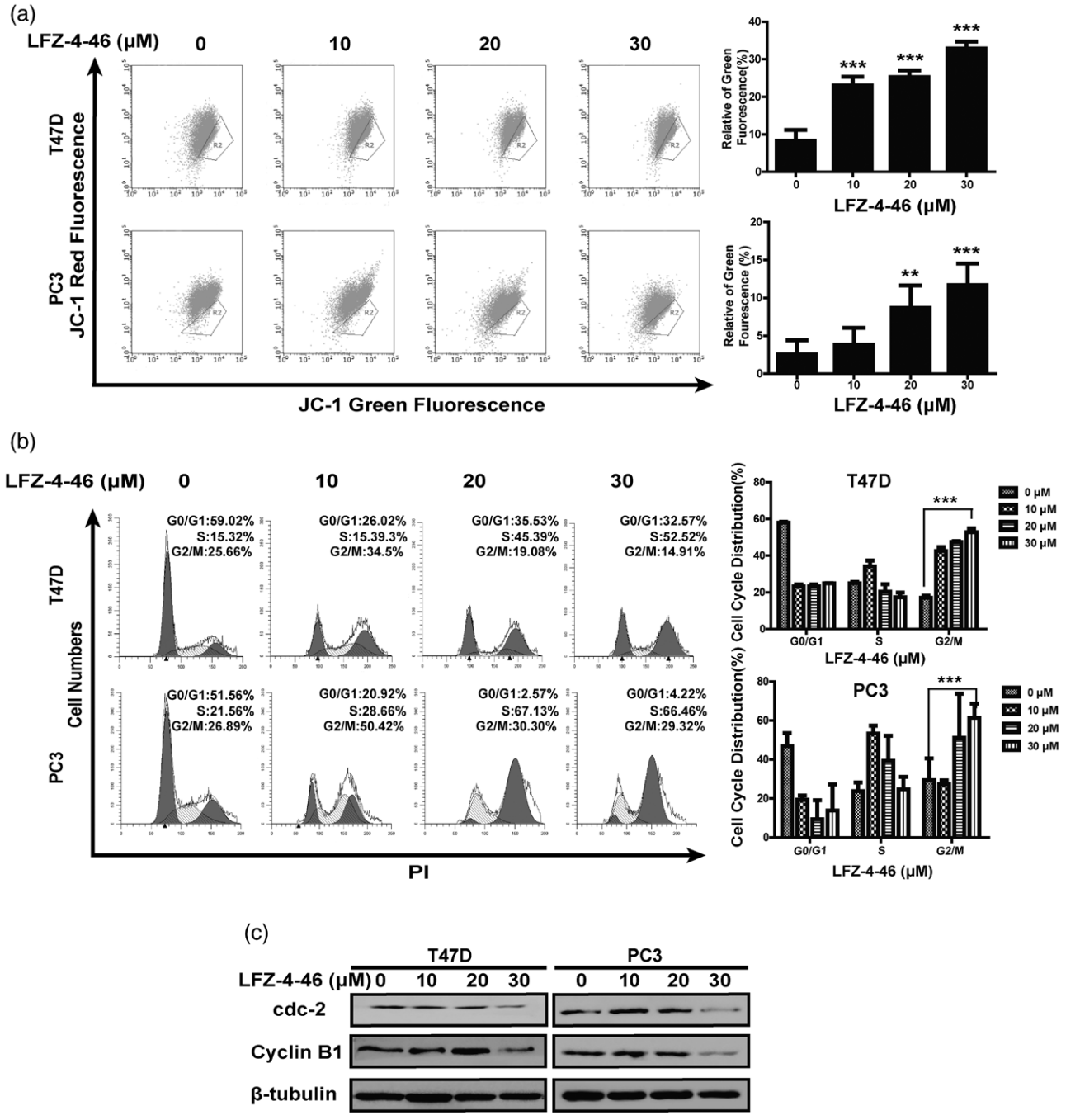

[2-hydroxy-1-phenyl-1,5,6,10b-tetrahydropyrazolo(5,1-a)isoquinolin-3(2*H*)-yl](phenyl) (LFZ-4-46) induced cell death by disrupting mitochondrial membrane potential (MMP) and arresting cell cycle. (a) Effect of LFZ-4-46 on MMP in T47D and PC3 cells was analyzed by flow cytometry after JC-1 staining. (b) After propidium iodide staining, the index of cell cycle was analyzed by flow cytometry. (c) Western blotting analyzed the cell cycle-related proteins in T47D and PC3 cells. Data are presented as the mean±SD of at least three independent experiments. ** $P<0.01$ *** $P<0.001$.

two cell lines were then chosen in the following studies. At the same time, LFZ-4-46 had a lower inhibitory effect on the viability of MCF-10A cells (IC_{50}>50 μM) (Table 1). Then, the effect of LFZ-4-46 on these two cell lines at different time point was investigated. As shown in Table 2 and Fig. 1d, LFZ-4-46 significantly inhibited the viability in a dose- and time-dependent manner. The above results suggested that LFZ-4-46 could significantly inhibit the growth of cancer cells in a time- and dose-dependent manner and have selective cytotoxicity to cancer cells.

Fig. 4

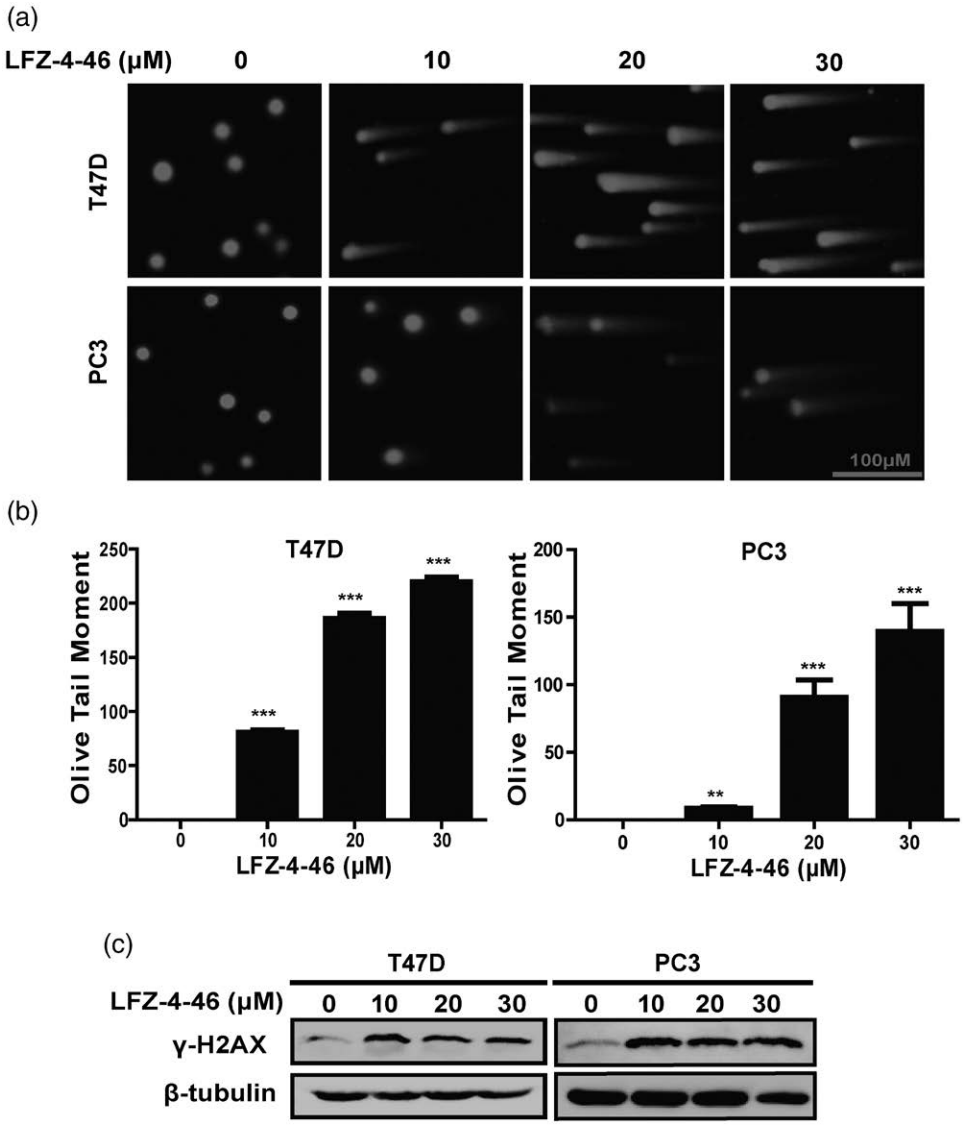

[2-hydroxy-1-phenyl-1,5,6,10b-tetrahydropyrazolo(5,1-a)isoquinolin-3(2*H*)-yl](phenyl) (LFZ-4-46) induced DNA damage in T47D and PC3 cells. (a) Representative images of LFZ-4-46-induced DNA damage (strand breaks) in T47D and PC3 cells were investigated by the comet assay (200× magnification). (b) The quantification of LFZ-4-46-induced DNA damage (strand breaks) images in T47D and PC3 cells by the comet assay software (CASP). (c) Western blotting analyzed the expression levels of γ-H2AX (Ser-139). Data are presented as the mean ± SD for at least three independent experiments. **P*<0.05, ***P*<0.01, *** *P*<0.001.

LFZ-4-46-induced apoptosis of cancer cells

To explore whether LFZ-4-46-inhibited cell viability was associated with apoptosis, both the cell lines were treated with LFZ-4-46 and stained with Annexin V-FITC/7AAD. As shown in Fig. 2a, LFZ-4-46 induced apoptosis in both cell lines in a dose-dependent manner. As the dose of LFZ-4-46 increased from 10 to 30 μM, the apoptosis rate of T47D and PC3 cells increased from 6.58 to 25.17% and 5.29 to 21.17%, respectively. DAPI staining was also involved to detect apoptosis. Nuclear DNA condensation and apoptotic bodies increased significantly after LFZ-4-46 treatment (Fig. 2b). Then, we examined the expression of apoptosis-related proteins by western blotting assay. As shown in Fig. 2c, LFZ-4-46 significantly induced the expression of cleaved caspase-3/7/9 and cleaved PARP and downregulated the expression of caspase-8 in T47D and PC3 cells. To further investigate whether LFZ-4-46-induced apoptosis was caspase-dependent, the effect of caspase inhibitor Z-VAD-FMK was introduced. Cotreatment with Z-VAD-FMK partially reversed the proportion of cell apoptosis and the expression of cleaved caspase-7 as respectively shown by flow cytometer and western blotting analysis, suggesting that the apoptosis induced by LFZ-4-46 was in a caspase-dependent manner (Fig. 2d–e).

Fig. 5

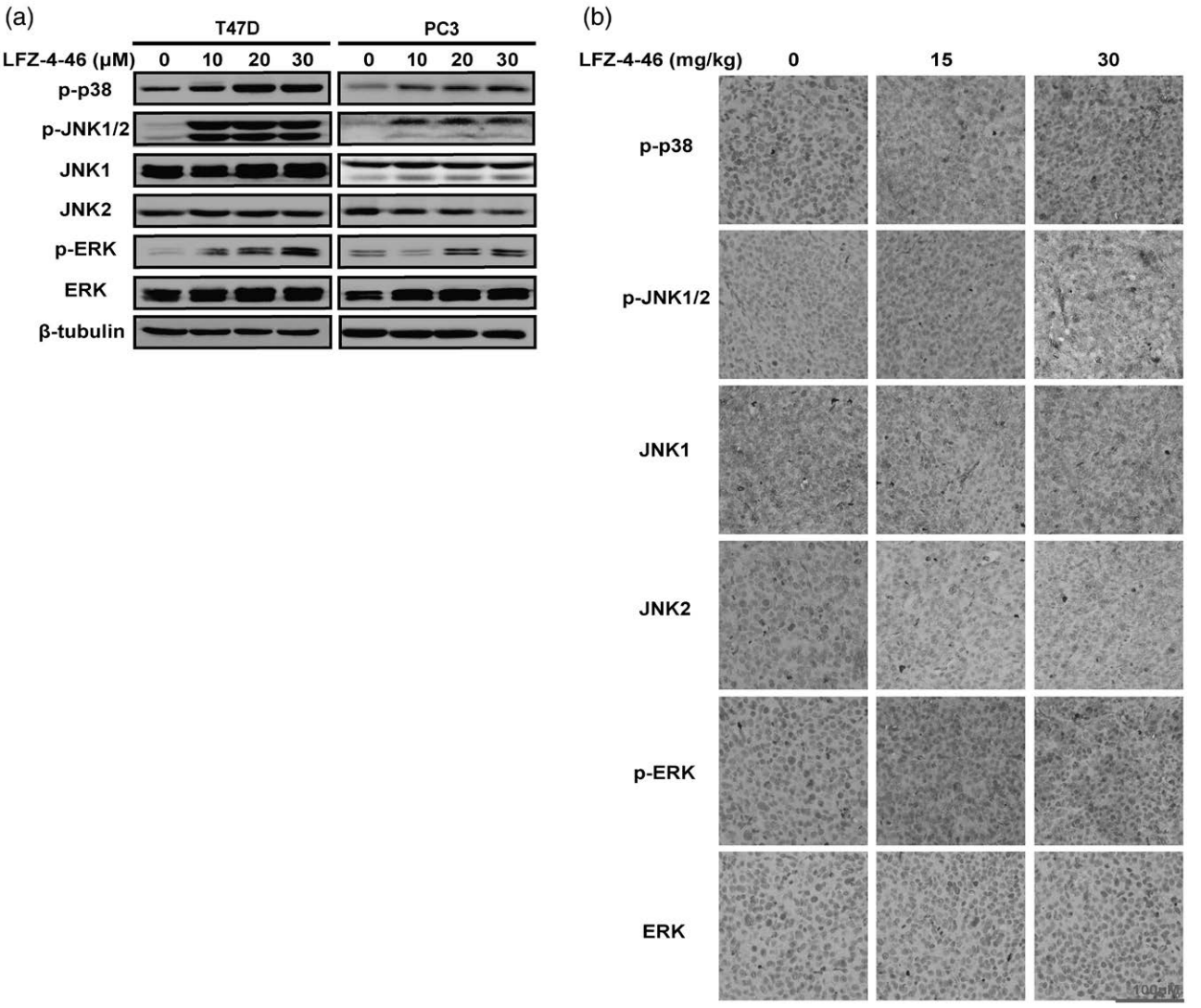

[2-hydroxy-1-phenyl-1,5,6,10b-tetrahydropyrazolo(5,1-a)isoquinolin-3(2*H*)-yl](phenyl) (LFZ-4-46) activated the mitogen-activated protein kinases (MAPKs) pathway. (a) The MAPKs pathway-related proteins in T47D and PC3 cells were detected by western blotting. (b) Immunohistochemistry was performed to detect the expression of ERK1/2, p-ERK1/2, JNK1/2, p-JNK1/2 and p-p38 in tumor tissues.

Mitochondria is important to the intrinsic apoptosis pathway. Mitochondrial membrane potential (MMP; $\Delta\psi m$) is considered to be a marker of apoptosis that occurs before caspase activation [18]. As shown in Fig. 3a, in both cell lines, LFZ-4-46 caused a sharp loss in MMP compared with the control group, and the relative percentages of low MMP in LFZ-4-46-treated T47D and PC3 cells increased by 2 times and 2.59 times, respectively. These results indicated that LFZ-4-46 induced mitochondria-mediated apoptosis and thus led to cell death, characterized by changes in MMP and activation of the caspase pathway.

LFZ-4-46-induced DNA damage

The signs of DNA damage are the phosphorylation of ser-139 residues of H2AX (γ-H2AX) [19]. After DNA damage, cells activate a series of complex signaling networks for DNA repair and apoptosis [20]. To further confirm whether LFZ-4-46-induced apoptosis was mediated by DNA damage, comet assay was used to detect the effect of LFZ-4-46 on T47D and PC3 cells. The results showed that compared with the control group, significant DNA double bond breakage occurred in the LFZ-4-46-treated group (Fig. 4a and b). Meanwhile, after LFZ-4-46 treatment, the expression of γ-H2AX was upregulated (Fig. 4c). The results showed that LFZ-4-46 could induce DNA damage in T47D and PC3 cells.

LFZ-4-46-induced cell cycle arrest

DNA damage activates checkpoints, delays cell cycle progression and triggers DNA repair [21]. We hypothesize

Fig. 6

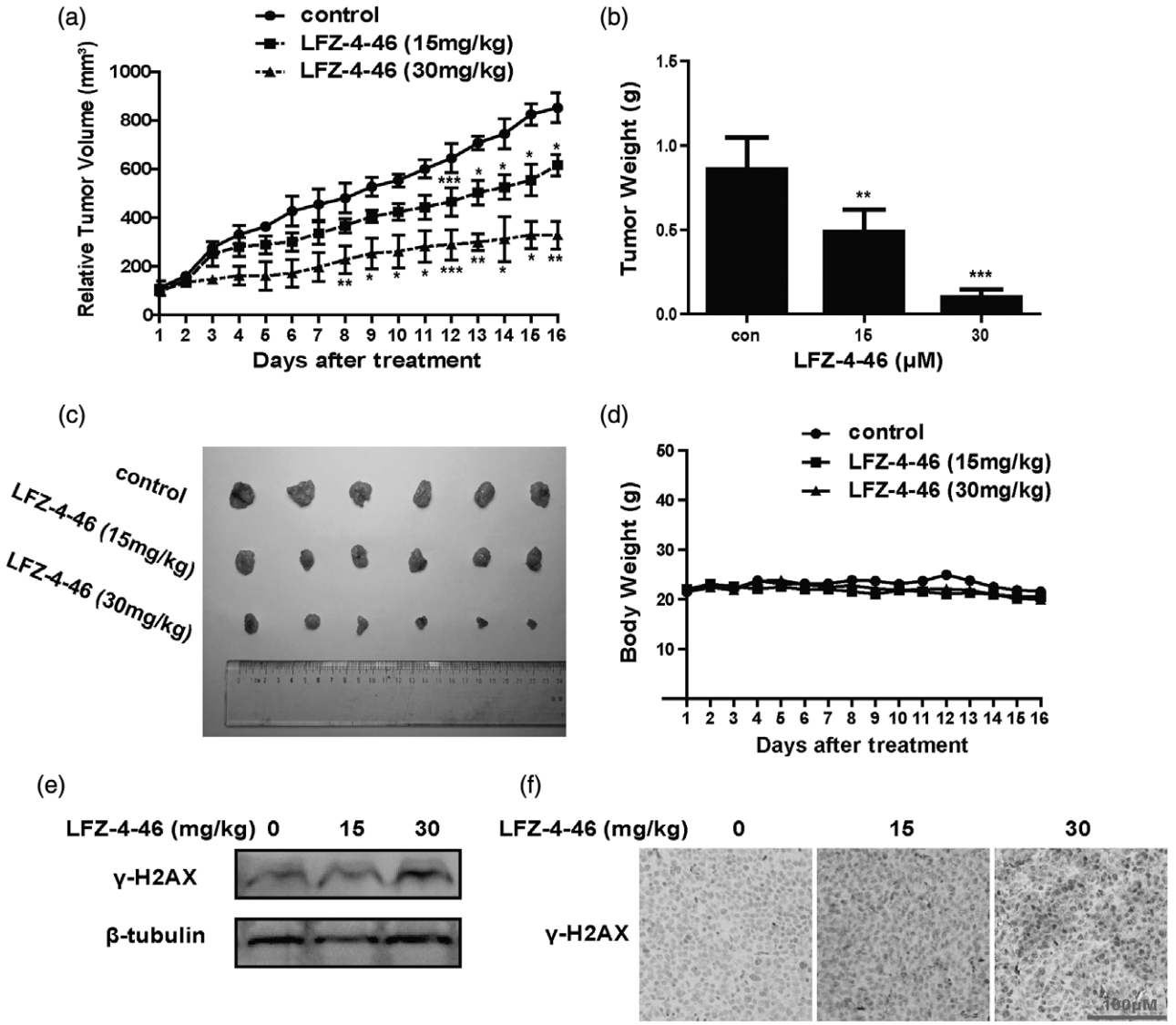

[2-hydroxy-1-phenyl-1,5,6,10b-tetrahydropyrazolo(5,1-a)isoquinolin-3(2H)-yl](phenyl) (LFZ-4-46) inhibited prostate cancer growth in vivo. (a)Tumor sizes were recorded every other day by vernier caliper measurements and calculated. (b) The average body weight of mice with xenografts was consecutively recorded. (c) After the mice were sacrificed, tumors were removed and photographed. Representative tumor images wereshown. (d) Tumor masses were weighted. (e) The expression of -H2AX (Ser-139) was analyzed by western blotting. (f) immunohistochemical wasper formed to detect the expression of -H2AX in tumor tissues. Data are expressed as mean SD. **P*<0.05, ***P*<0.01, ****P*<0.001.

that LFZ-4-46 causes cell cycle arrest through DNA damage. Cell cycle progression was examined by flow cytometry. The results showed that LFZ-4-46 could significantly arrest cell cycle at the G2/M phase (Fig. 3b). Consistent with the above results, western blotting results showed the expression levels of cdc-2 and Cyclin B1 were significantly down-regulated, after treatment with LFZ-4-46 (Fig. 3c). The above results suggested that LFZ-4-46 induced cell cycle arrest at the G2/M phase in both cancer cells.

LFZ-4-46 activated mitogen-activated protein kinases pathway

The apoptotic pathway includes the MAPKs pathway [22]. A series of studies have reported that the induction of cell apoptosis is associated with DNA damage response pathway and the MAPKs pathway [23,24]. Furthermore, these pathways are involved in the cellular responses, such as cell proliferation, migration, apoptosis and cell cycle [25]. In this experiment, it was proved that the lead compound LFZ-4-46 could induce cell apoptosis and

Fig. 7

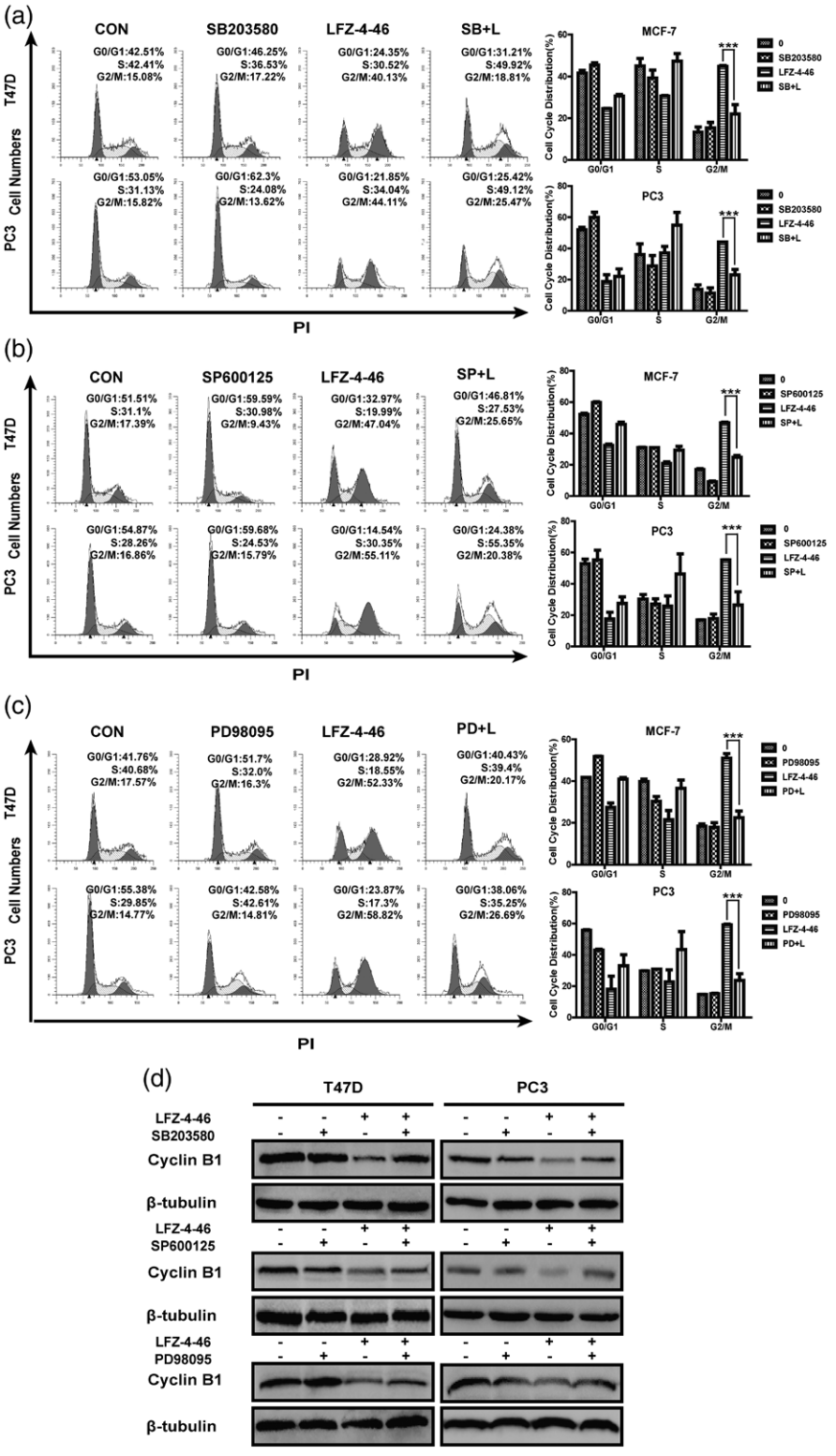

[2-hydroxy-1-phenyl-1,5,6,10b-tetrahydropyrazolo(5,1-a)isoquinolin-3(2H)-yl](phenyl) (LFZ-4-46) induced cell cycle arrest by activating themitogen-activated protein kinases (MAPKs) pathway. T47D and PC3 cells were treated with LFZ-4-46 (30 M) for 24 h after pretreatment withSB203580 (25 M) (a), SP600125 (30 M) (b), and PD98095 (50 M) (c) for 2 h. After propidium iodide staining, the index of cell cycle wasanalyzed by flow cytometry. (d) The expression levels of Cyclin B1 were analyzed by western blotting. Data are presented as the meanSD forthree independent experiments. ***$P<0.001$

Fig. 8

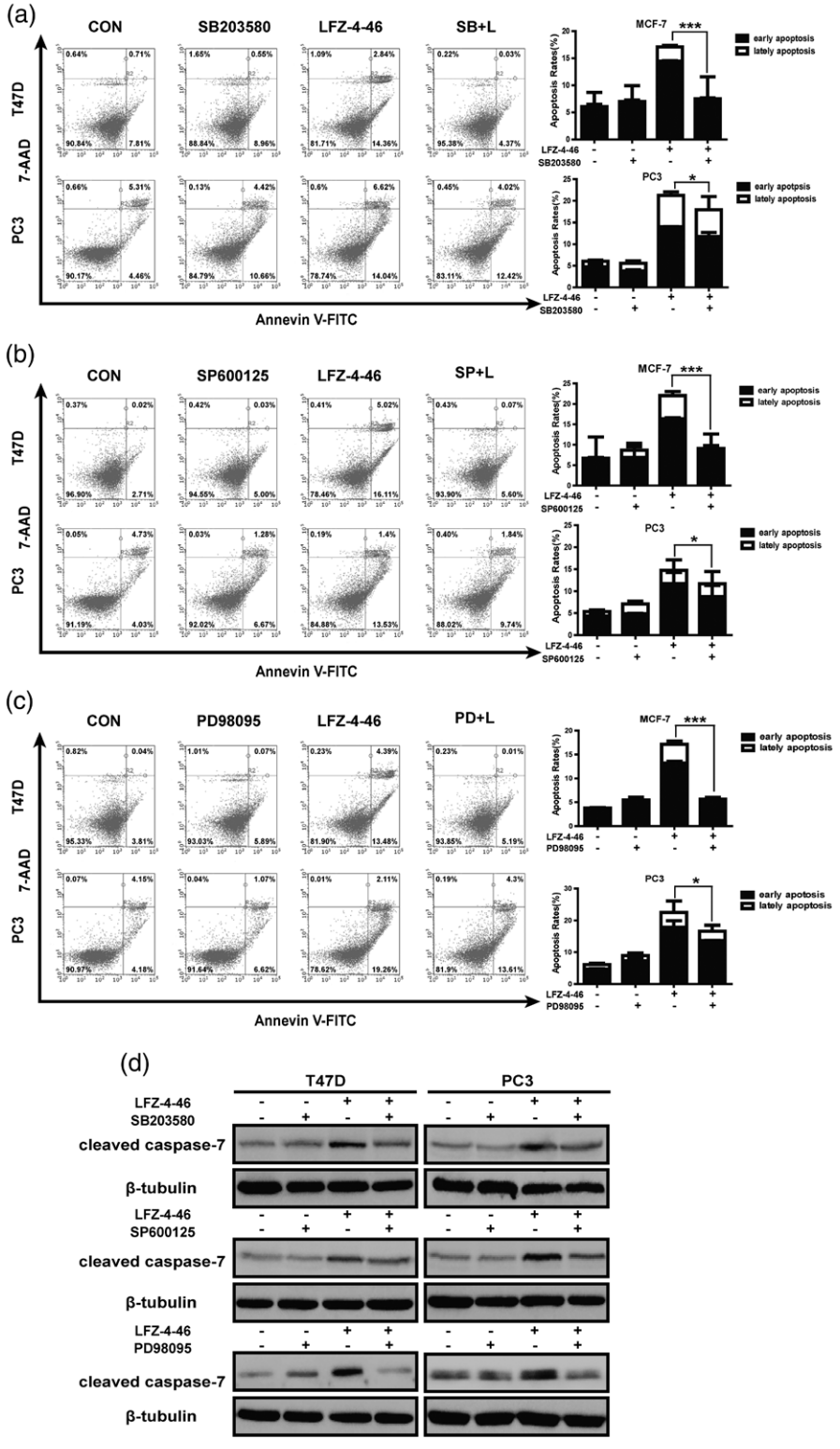

[2-hydroxy-1-phenyl-1,5,6,10b-tetrahydropyrazolo(5,1-a)isoquinolin-3(2H)-yl](phenyl) (LFZ-4-46) induced cell apoptosis by activating themitogen-activated protein kinases (MAPKs) pathway. T47D and PC3 cells were treated with LFZ-4-46 (30M) for 24h after pretreatment with SB203580 (25M) (a), SP600125 (30M) (b) and PD98095 (50M) (c) for 2h. After Annexin V-fluorescein isothiocyanate (FITC)/7AAD staining, the index of apoptotic cells was analyzed by flow cytometry. (d) The expression levels of cleaved caspase-7 were analyzed by western blotting.Data are presented as the mean SD of three independent experiments. *P<0.05, ***P<0.001.

DNA damage. We hypothesize that LFZ-4-46 causes cell apoptosis through the MAPKs pathway by targeting JNK, p38 and ERK pathways. For this, LFZ-4-46 treated with the concentration of 10, 20 and 30 μM in T47D and PC3 cells for 24 h, which was followed by western blotting and flow cytometry analysis. As shown in Fig. 5a, the total protein expression was not obviously altered but phosphorylation of JNK, p38 and ERK was induced. To further investigate whether the MAPKs pathway was involved in the cell apoptosis and cell cycle arrest induced by LFZ-4-46, the MAPKs pathway inhibitors SB203580 (the p38/MAPK inhibitor), SP600125 (the c-Jun-N-terminal kinase inhibitor) and PD98095 (the MAPK/ERK inhibitor) were introduced. When pretreated with the inhibitors, LFZ-4-46-induced cell apoptosis and cell cycle arrest were attenuated (Figs. 7 and 8). The results indicated that LFZ-4-46 induced cell apoptosis and cell cycle arrest by activating MAPKs pathways.

LFZ-4-46 inhibited tumor growth in a mouse Xenograft tumor model

In order to further assess the effects of LFZ-4-46 on tumor growth *in vivo*, a xenograft nude mice model of PC3 cells was established. PC3 cells (5×10^6) were inoculated in the flank of BALB/c male nude mice. As shown in Fig. 6a–c, the tumor volume and weight were significantly suppressed in the LFZ-4-46-treated groups. In addition, there was no obvious body weight loss of mice during the whole process, which means that LFZ-4-46 has no obvious toxicity (Fig. 6d). Compared with the control group, the immunohistochemical analysis and western blotting assays showed that LFZ-4-46 significantly reduced the expression of γ-H2AX in the tumor tissue sections (Fig. 6e–f). To further detect whether the MAPKs pathway was involved *in vivo*, the expression of ERK1/2, p-ERK1/2, JNK1/2, p-JNK1/2 and p-p38 was detected by immunohistochemical staining. Compared with the control group, the phosphorylation of JNK, p38 and ERK was increased but the total protein expression was not obviously altered (Fig. 5b). These data indicated that LFZ-4-46 can inhibit tumor growth through inducing DNA damage and activating the MAPKs pathway *in vivo*.

Discussion

Cancer is one of the highest incidences of malignant tumors in the world that it is urgent to find a new agent to treat. In the present study, we demonstrated that LFZ-4-46 exhibited significantly inhibitory effect on the vitality of cancer cells.

DNA damage occurs on exposure to genotoxic agents and during physiological DNA transactions [26]. DNA strand break is the main form of DNA damage [27]. In this study, the comet assay detected the DNA strand break and western blotting analysis showed the increase of γ-H2AX (a biomarker of DNA damage) expression, indicating that LFZ-4-46 induced DNA damage in T47D and PC3 cells (Fig. 4). Meanwhile, there is a piece of evidence that DNA damage can induce cell apoptosis [28]. Consistent with the above notion, in the present study, we found that LFZ-4-46 treatment resulted in significant induction of apoptosis in T47D and PC3 cells accompanied with the DNA damage occurs (Fig. 2a–c). Meanwhile, loss of the MMP ($\Delta\psi m$) is a sign of early apoptosis [29] and the activation of the caspase family is known to play an important role in cancer cell apoptosis. After LFZ-4-46 treatment, the disruption of MMP (Fig. 3a) and the activation of claved-caspase-3/7/9 were observed in T47D and PC3 cells (Fig. 2c). In addition, the caspase-dependent apoptosis induced by LFZ-4-46 was reversed with treatment by the caspase inhibitor Z-VAD-FMK (Fig. 2d–e). Thereby, LFZ-4-46-mediated cell apoptosis is characterized by loss of MMP and activation of caspases. These findings suggest that LFZ-4-46-induced apoptosis of T47D and PC3 cells may be activated by DNA damage. At the same time, once DNA damage occurs in cells, the cell cycle checkpoints will immediately be activated, which leads to cell cycle arrest at the G2/M phase, providing sufficient time for the orderly DNA repair process [30,31]. In this study, we found that LFZ-4-46 induced cell cycle arrested at the G2/M phase and downregulated the related protein expression of cdc2 and Cyclin B1 (Fig. 3b–c).

In physiological and pathological processes, it is known that the MAPKs are involved in cell growth, cell cycle and apoptosis [32]. As shown in Fig. 5, we identified that LFZ-4-46 activated p38/JNK/ERK phosphorylation. The proportion of cell apoptosis and cell cycle arrest were significantly attenuated after treatment with the MAPKs pathway inhibitors SB203580, SP600125 and PD98095 (Figs. 7 and 8). These indicated that LFZ-4-46-induced apoptotic cell death and cell cycle arrest might be via the activation of MAPKs pathway.

In summary, we found that LFZ-4-46, a lead compound, had an effective growth-inhibitory effect on the proliferation of the cancer cells *in vitro* and *in vivo* through inducing DNA damage and activating the MAPKs pathway. In this study, we have initially explored the effect of LFZ-4-46. In addition, the detailed molecular mechanisms of LFZ-4-46-induced DNA damage and activation of MAPKs pathway are worthy to be studied in the future.

Conclusion

LFZ-4-46, a tetrahydroisoquinoline derivative with a pyrazolidine moiety, has a good anticancer activity. In this study, we found that LFZ-4-46 could effectively inhibit the viability of different human cancer cells. Related mechanistic studies have found that LFZ-4-46 activated caspase-dependent apoptosis pathway, led to cell cycle arrest at the G2/M phase through induction of DNA

damage and activation of MAPKs pathway *in vitro* and *in vivo*. In short, our data suggest that LFZ-4-46 may be a novel lead compund for the treatment of breast and prostate cancer.

Acknowledgements

This study was supported by the National Natural Science Foundation of China (grants no. 81774003), the Zhejiang Provincial Natural Science Fund (LQ19H160006) and the Zhejiang Chinese Medical University Research Fund Project (KC201912 and 2018ZZ09).

Conflicts of interest

There are no conflicts of interest.

References

1 DeSantis CE, Ma J, Gaudet MM, Newman LA, Miller KD, Goding Sauer A, *et al*. Breast cancer statistics, 2019. *CA Cancer J Clin* 2019; **69**:438–451.
2 Barzilai A, Yamamoto K. DNA damage responses to oxidative stress. *DNA Repair (Amst)* 2004; **3**:1109–1115.
3 Global Burden of Disease Cancer C, Fitzmaurice C, Dicker D, Pain A, Hamavid H, Moradi-Lakeh M, *et al*. The global burden of cancer 2013. *JAMA Oncol* 2015; **1**:505–527.
4 Rosenberg J, Ischebeck T, Commichau FM. Vitamin B6 metabolism in microbes and approaches for fermentative production. *Biotechnol Adv* 2017; **35**:31–40.
5 Katoh T, Tomata Y, Setoh M, Sasaki S, Takai T, Yoshitomi Y, *et al*. Practical application of 3-substituted-2,6-difluoropyridines in drug discovery: facile synthesis of novel protein kinase C theta inhibitors. *Bioorg Med Chem Lett* 2017; **27**:2497–2501.
6 Constable EC, Housecroft CE, Neuburger M, Phillips D, Raithby PR, Schofield E, *et al*. Development of supramolecular structure through alkylation of pendant pyridyl functionality. *J Chemical Society Dalton Transactions* 2000:2219–2228.
7 Capilla AS, Soucek R, Grau L, Romero M, Rubio-Martínez J, Caignard DH, Pujol MD. Substituted tetrahydroisoquinolines: synthesis, characterization, antitumor activity and other biological properties. *Eur J Med Chem* 2018; **145**:51–63.
8 Strongb KL, Epplinb MP, Bacsab J, Butchb CJ, Burgerb PB, Menaldinob DS, *et al*. The structure activity relationship of a tetrahydroisoquinoline class of N-Methyl-D-Aspartate receptor modulators that potentiates GluN2B-containing N-Methyl-D-aspartate receptors. *J Med Chem* 2017; **13**:5556–5585.
9 Li YS, Liu XY, Zhao DS, Liao YX, Zhang LH, Zhang FZ, *et al*. Tetrahydroquinoline and tetrahydroisoquinoline derivatives as potential selective PDE4B inhibitors. *Bioorg Med Chem Lett* 2018; **28**:3271–3275.
10 Scott JD, Williams RM. Chemistry and biology of the tetrahydroisoquinoline antitumor antibiotics. *Chem Rev* 2002; **102**:1669–1730.
11 Li D, Yang D, Wang L, Liu X, Wang K, Wang J, *et al*. An efficient nickel-catalyzed asymmetric oxazole-forming ugi-type reaction for the synthesis of chiral aryl-substituted THIQ rings. *Chemistry* 2017; **23**:6974–6978.
12 Martens T, Sengmany S, Ollivier A, Rey M, Léonel E. Direct Phosphonylation of N-Carbamate-tetrahydroisoquinoline by convergent paired electrolysis. *Synlett* 2020; **31**:1191–1196.
13 Perepichka I, Kundu S, Hearne Z, Li CJ. Efficient merging of copper and photoredox catalysis for the asymmetric cross-dehydrogenative-coupling of alkynes and tetrahydroisoquinolines. *Org Biomol Chem* 2015; **13**:447–451.
14 Zeng L, Huang B, Shen Y, Cui S. Multicomponent synthesis of tetrahydroisoquinolines. *Org Lett* 2018; **20**:3460–3464.
15 Ahn JH, Kim JA, Kim HM, Kwon HM, Huh SC, Rhee SD, *et al*. Synthesis and evaluation of pyrazolidine derivatives as dipeptidyl peptidase IV (DP-IV) inhibitors. *Bioorg Med Chem Lett* 2005; **15**:1337–1340.
16 Gilbert AM, Failli A, Shumsky J, Yang Y, Severin A, Singh G, *et al*. Pyrazolidine-3,5-diones and 5-hydroxy-1H-pyrazol-3(2H)-ones, inhibitors of UDP-N-acetylenolpyruvyl glucosamine reductase. *J Med Chem* 2006; **49**:6027–6036.
17 Surendra Kumar R, Moydeen M, Al-Deyab SS, Manilal A, Idhayadhulla A. Synthesis of new morpholine-connected pyrazolidine derivatives and their antimicrobial, antioxidant, and cytotoxic activities. *Bioorg Med Chem Lett* 2017; **27**:66–71.
18 Galluzzi L, Vanden Berghe T, Vanlangenakker N, Buettner S, Eisenberg T, Vandenabeele P, *et al*. Programmed necrosis from molecules to health and disease. *Int Rev Cell Mol Biol* 2011; **289**:1–35.
19 Mah LJ, El-Osta A, Karagiannis TC. gammaH2AX: a sensitive molecular marker of DNA damage and repair. *Leukemia* 2010; **24**:679–686.
20 Hafner A, Bulyk ML, Jambhekar A, Lahav G. The multiple mechanisms that regulate p53 activity and cell fate. *Nat Rev Mol Cell Biol* 2019; **20**:199–210.
21 Chao HX, Poovey CE, Privette AA, Grant GD, Chao HY, Cook JG, Purvis JE. Orchestration of DNA damage checkpoint dynamics across the human cell cycle. *Cell Syst* 2017; **5**:445–459.e5.
22 Yue J, Lopez JM. Understanding MAPK signaling pathways in apoptosis. *Int J Mol Sci* 2020; **21**:2346.
23 Dai Y, Chen S, Pei XY, Almenara JA, Kramer LB, Venditti CA, *et al*. Interruption of the Ras/MEK/ERK signaling cascade enhances Chk1 inhibitor-induced DNA damage *in vitro* and *in vivo* in human multiple myeloma cells. *Blood* 2008; **112**:2439–2449.
24 Surova O, Zhivotovsky B. Various modes of cell death induced by DNA damage. *Oncogene* 2013; **32**:3789–3797.
25 Tutuka CSA, Andrews MC, Mariadason JM, Ioannidis P, Hudson C, Cebon J, Behren A. PLX8394, a new generation BRAF inhibitor, selectively inhibits BRAF in colonic adenocarcinoma cells and prevents paradoxical MAPK pathway activation. *Mol Cancer* 2017; **16**:112.
26 Bednarski JJ, Sleckman BP. At the intersection of DNA damage and immune responses. *Nat Rev Immunol* 2019; **19**:231–242.
27 Pelicano H, Carney D, Huang P. ROS stress in cancer cells and therapeutic implications. *Drug Resist Updat* 2004; **7**:97–110.
28 Soták M, Sumová A, Pácha J. Cross-talk between the circadian clock and the cell cycle in cancer. *Ann Med* 2014; **46**:221–232.
29 Jeong SY, Seol DW. The role of mitochondria in apoptosis. *BMB Rep* 2008; **41**:11–22.
30 Shen Y, Sherman JW, Chen X, Wang R. Phosphorylation of CDC25C by AMP-activated protein kinase mediates a metabolic checkpoint during cell-cycle G2/M-phase transition. *J Biol Chem* 2018; **293**:5185–5199.
31 Bensimon A, Aebersold R, Shiloh Y. Beyond ATM: the protein kinase landscape of the DNA damage response. *FEBS Lett* 2011; **585**:1625–1639.
32 Sun H, Ou B, Zhao S, Liu X, Song L, Liu X, *et al*. USP11 promotes growth and metastasis of colorectal cancer via PPP1CA-mediated activation of ERK/MAPK signaling pathway. *Ebiomedicine* 2019; **48**:236–247.